Mechanical Testing and Diagnosis
ISSN 2247 – 9635, 2012 (II), Volume 4, 68-75

HEAT INDUCTION TREATMENT AND THE BALL DIAMETER LIMITATION IN POINT CONTACT SLEWING RINGS

Daniel REZMIRES[1], Alfredo MONFARDINI[2], Cezar RACOCEA[3]

[1] S.C. SIRCA S.A, Piatra Neamt, ROMANIA, [2] RIMA Spa., ITALY,
[3] Technical University "Gh. Asachi"- Iasi, ROMANIA

- drezmir@hotmail.com; sirca.com.ro, www.rimaspa.it, cracocea@netscape.net

ABSTRACT

The static and dynamic load capacity in slewing rings depends on the contact geometry and the surface and subsurface hardening parameter. Usually, for the large diameter slewing rings, the raceway treatment is the induction hardening. The specific depth varies between 1 mm to 8 mm, depending upon the hardening technique and the material composition and quality. In this paper, the surface and subsurface stresses will be examined taking into account the link between the ball diameter and the material structure using a hardness compression algorithm. This reflects the contact limitations induced by the ball diameter and shows two possible regions for crack initiations in this rolling contact.

Keywords: slewing rings, CIF (high frequency induction hardening), C45 steel grade, 42CrMo4 steel grade, Hertzian contact, non-Hertzian contact analysis, compression Jominy curve, ball diameter limitation

1. ANALYSIS

The rolling contact stresses and the quasi-static parameters discussed in the literature are considered as already known [1, 2]. The maximum shear stress below surface and its position are functions of the contact parameters, the friction coefficient and the film parameter Λ. Two different materials were chosen in this analysis, the steel grades C45 and 42CrMo4. The chemical composition of the two materials is presented below [3].

Table 1. Chemical composition of the steel grades

	C	Si	Mn	P	S	Cr	Mo	Ni	Cr+Mo+ Ni
C45	0.42-0.50	<0.40	0.50-0.80	<0.035	<0.035	<0.40	<0.10	<0.40	<0.63
42CrMo4	0.38-0.45	<0.40	0.60-0.90	<0.035	<0.035	0.90-1.20	0.15-0.30		

A compression hardening algorithm was applied for the specific Jominy curve, taking into account the inductor time passing and the inductor frequencies. Usually the deep hardness is given as function of time passing and working frequency by the following formula as $\delta(f,t)=8{,}5/f^{0.5}+2{,}4*t^{0.5}$ [5,6], where f represents the working machine frequency in kHz, and t is the time passing of the inductor piece in front a specific surface. According to [3, 4] the hardenability diagrams for C45 and 42CrMo4 are presented in Figure 1.

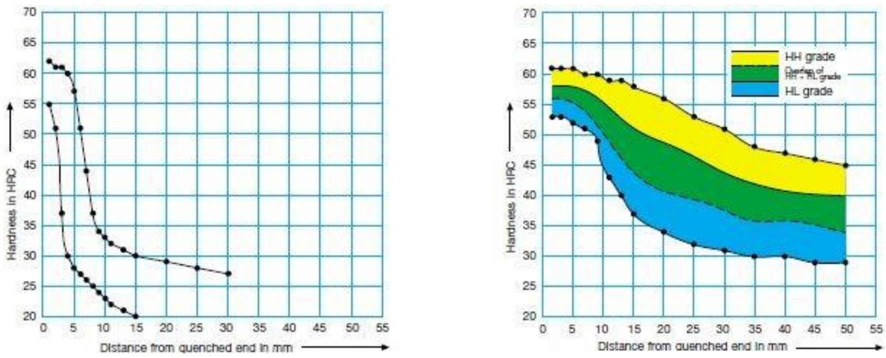

C45 hardenability diagram 42CrMo4 hardenability diagram

Fig. 1. Hardening diagram for C45 and 42CrMo4

Some interpolation functions were created to insert in computer the two Jominy curves and the results are presented in Figure 2 and Figure 3. RM=RM(HRC) and σ02=σ02(HRC) were also computed.

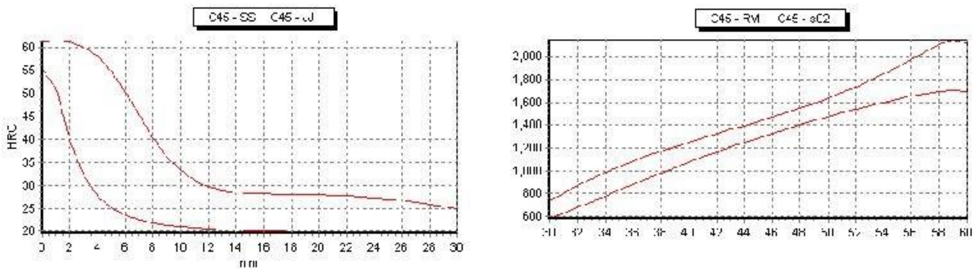

Modelled Jominy curve RM and σ02 as function of HRC

Fig. 2. Jominy, Rm and σ02 for C45

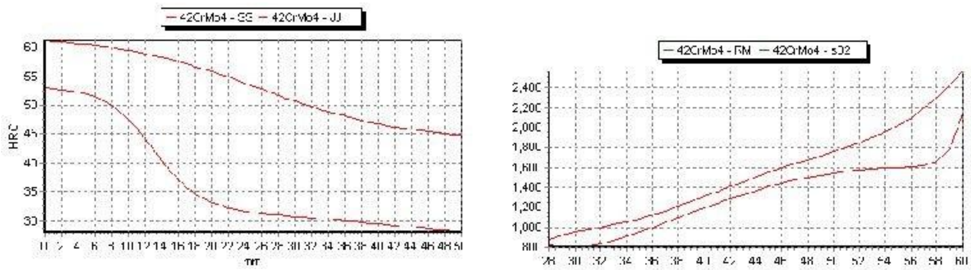

Modelled Jominy curve RM and σ02 as function of HRC

Fig. 3. Jominy, Rm and σ02 for 42CrMo4

With these initial data δ(f, t) and HRC=HRC (Jominy), a compressed Jominy curve is created by scaling the initial Jominy curve just to fit into δ(f,t) value. These data are presented in Fig. 4 as function of machine frequency for 2 seconds as passing time machine.

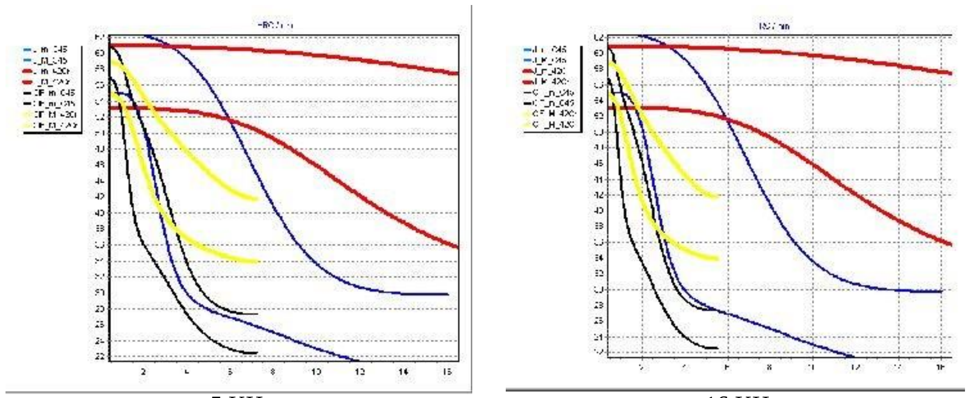

5 KHz 16 KHz

Fig. 4. Jominy curve and Compression algorithm

The theoretical hardening depth depends [5, 6] on the CIF (high frequency induction hardening)machine parameter (Fig. 5, [7, 8, 11]) and can be computed according to the process parameter.

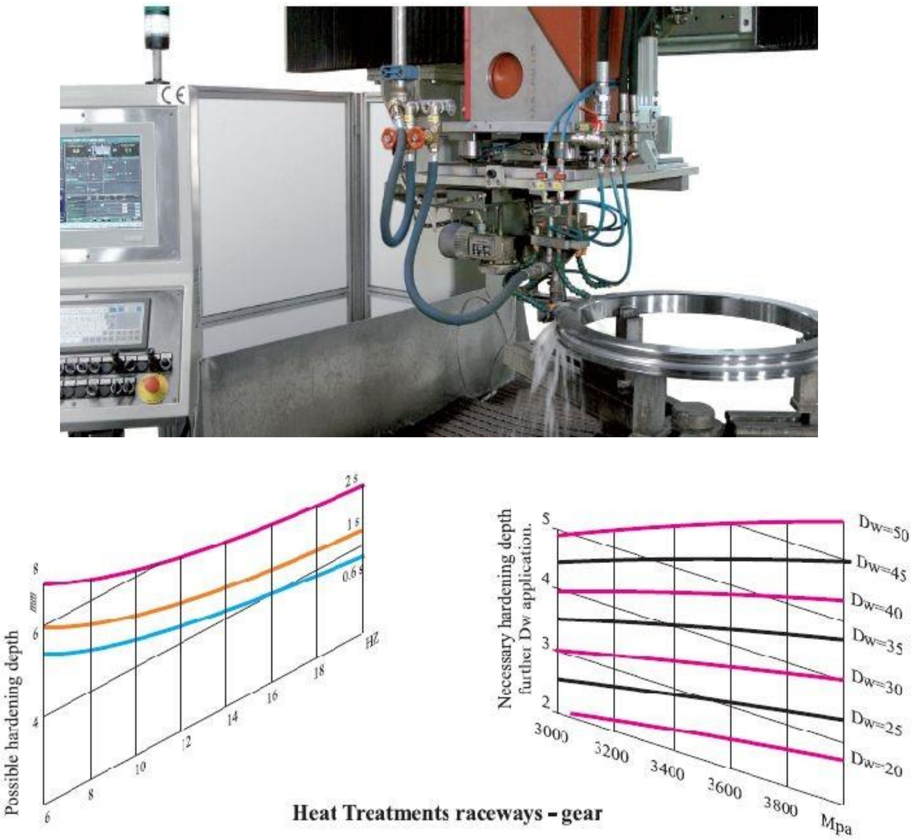

Fig. 5. CIF installation and hardness depth

Using the Hertz theory [1, 2], a computer code was developed [9] and the stress parameter was computed for quasi-static and quasi-dynamic cases and it results distributions with the following forms (Fig. 6 a, b, c, d, e and f) for Dw=20, f=0.52.

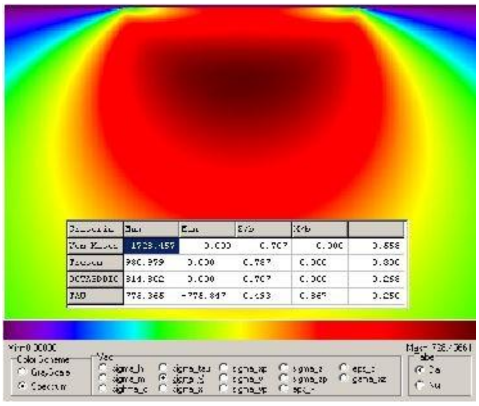

Fig 6.a – 0 friction coefficient

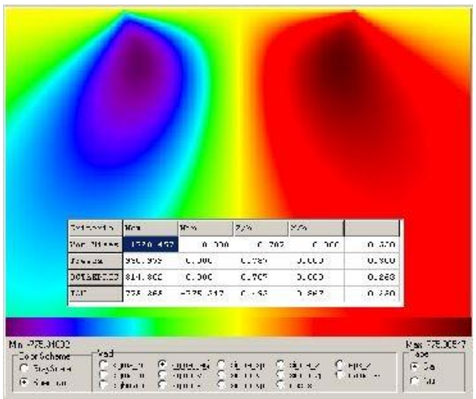

Fig 6.b – 0 friction coefficient

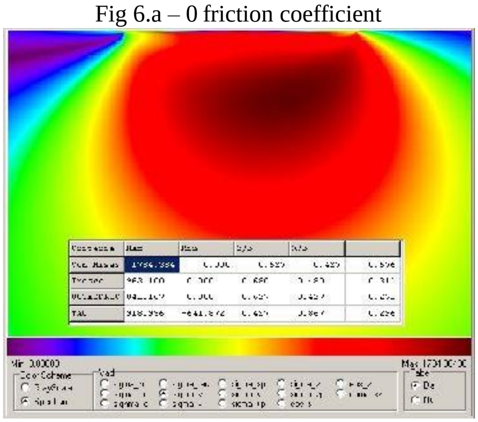

Fig 6.c – 0.15 friction coefficient effect

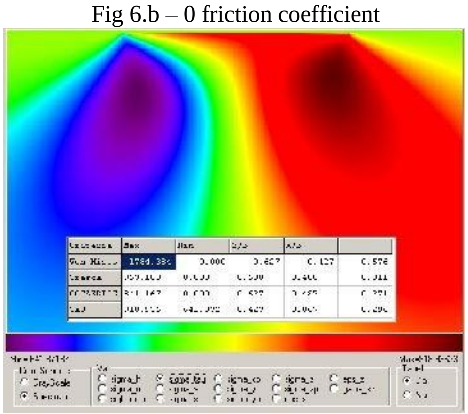

Fig 6.d – 0.15 friction coefficient effect

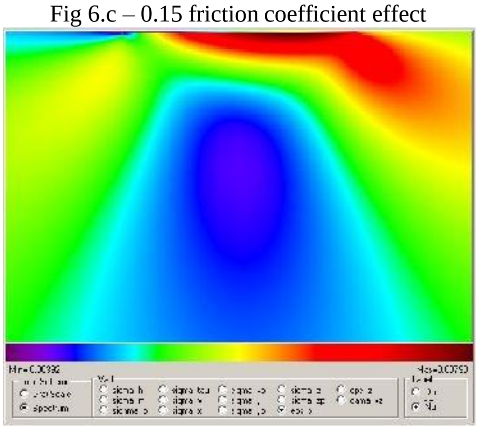

Fig 6.e – 0.15 friction coefficient effect

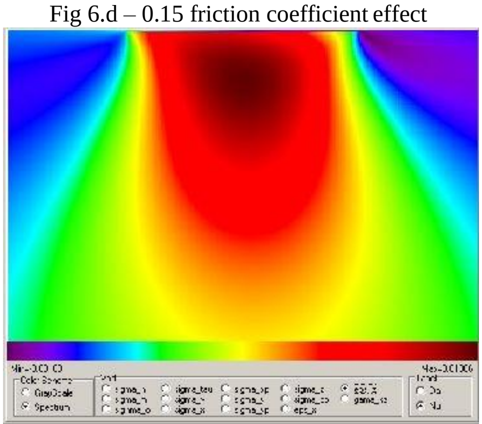

Fig 6.f – 0.15 friction coefficient effect

The contour of the stress given by contact stress analysis and the results from the compression algorithm were superimposed and one / two possible danger areas were revealed (Fig.) [7, 8], for two different values of the friction coefficient.

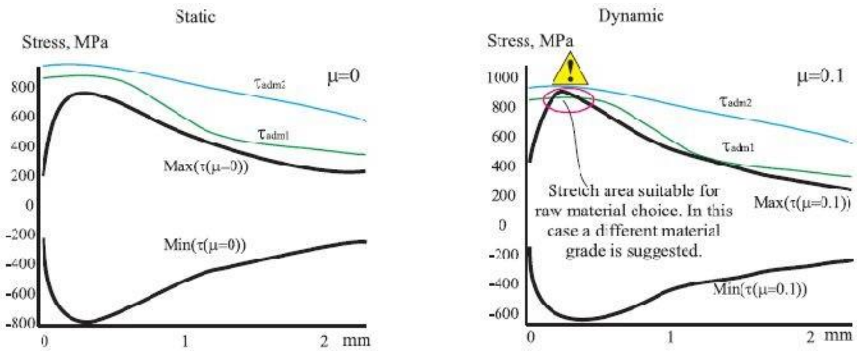

Fig. 7. Possible danger area for static and dynamic contact

The stretch area depends on the ball diameter, raceway conformity, hertzian or non Hertzian contact ellipse area (cutting or non cutting point contact) and from here results the obligation to choose another material for the same contact pressure value. Rm(HRC), σ02(HRC) as function of material and machine parameters for 2,5 mm for C45 and 42CrMo4 are exposed in figure 8, where the yellow curve is τ admissible.

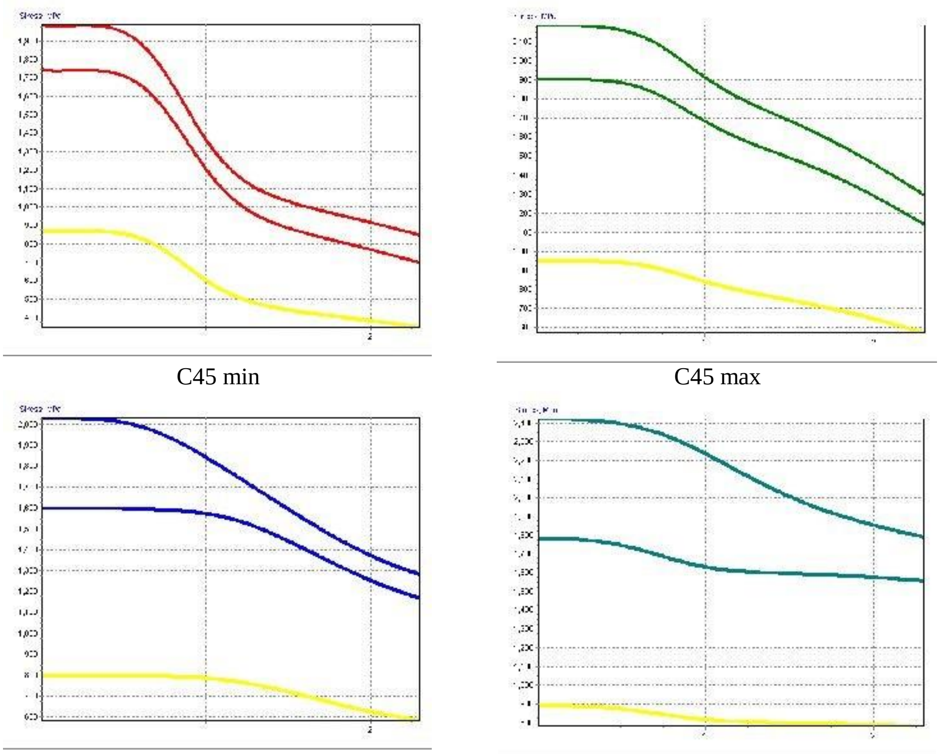

C45 min | C45 max

42CrMo4 min | 42CrMo4 max

Figure 8. The admissible values and Rm(HRC), σ02(HRC), τ admissible as function of material Jominy parameter

Figure 8 presents the Rm(HRC), σ02(HRC), τ for C45 min, C45 max, 42CrMo4 min and 42CrMo4 max, where “min” corresponds to HL grade and “max” corresponds to HH grade (see Fig. 1). For different ball diameters, it was compared sigma_tau (from Fig. 6) in depth with τ admissible on each layer along the direction surface -> depth (Fig. 8). That method was applied and static and dynamic analyses were performed considering the same contact pressure. From that analysis, it results one or two stretch areas, which have to be taken into account (see Fig. 9)

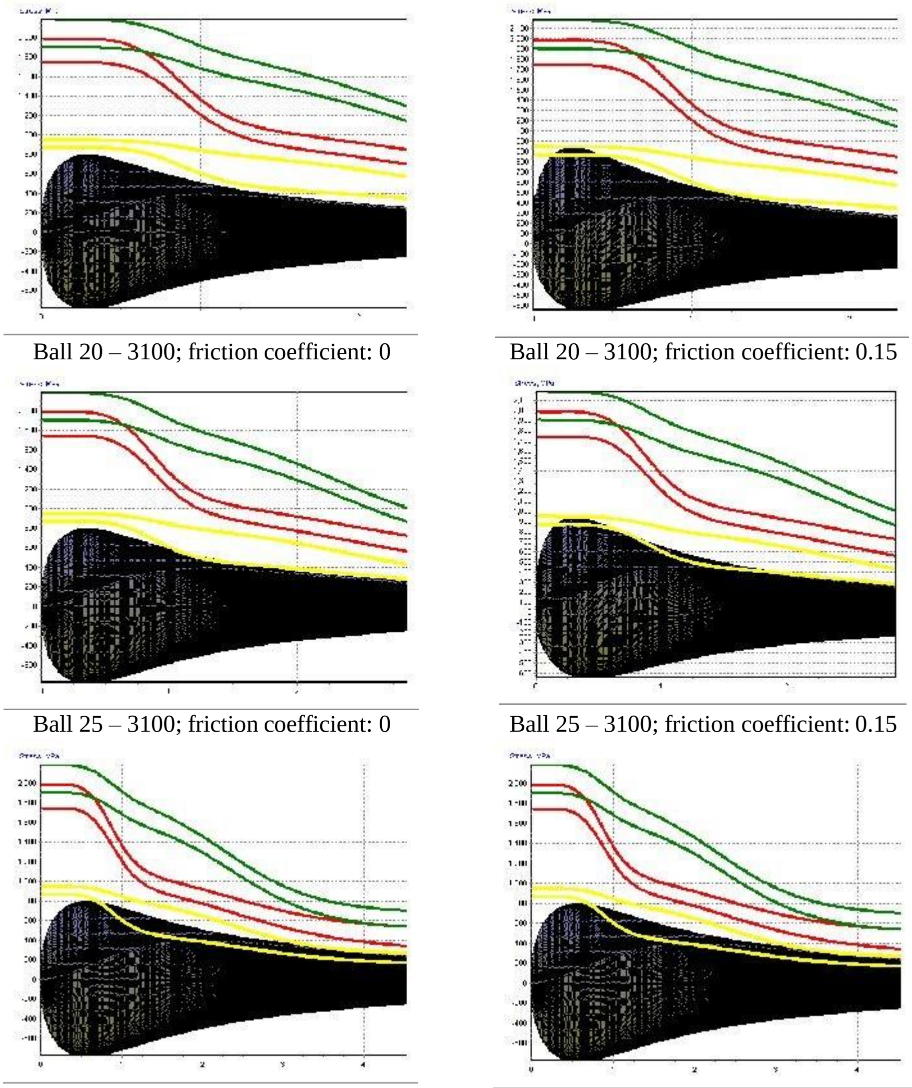

Ball 20 – 3100; friction coefficient: 0

Ball 20 – 3100; friction coefficient: 0.15

Ball 25 – 3100; friction coefficient: 0

Ball 25 – 3100; friction coefficient: 0.15

Ball 40 – 3100; friction coefficient: 0

Ball 40 – 3100; friction coefficient: 0.15

Fig. 9. Analysis for C45, sigma_tau, τ admissible, 16 KHz, f=0.52

If the grinding process is applied to a raceway, a small quantity of material is eliminated. Figure 10 shows this effect on C45 m, 16 KHz, f=0.52, Dw=20 mm for 0 mm and 0.31 mm deep of grinding process applied to a raceway. The same type of analysis is made for C45 max, 16 KHz, f=0.52, Dw=20 mm for 0 mm and 0.31 mm deep of grinding process applied to a raceway and the results are presented in Fig. 11.

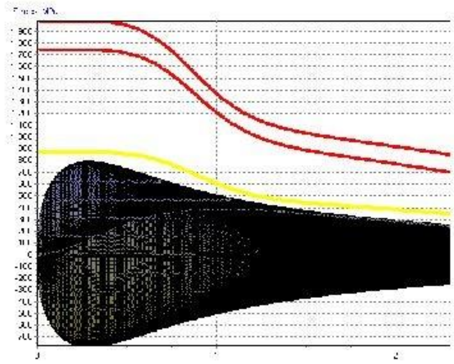

Sigma_tau and Rm(HRC), σ02(HRC), τ admissible for 0 mm – grinding

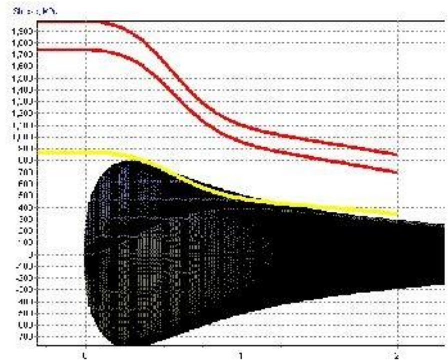

Sigma_tau and Rm(HRC), σ02(HRC), τ admissble for 0.31 mm – grinding

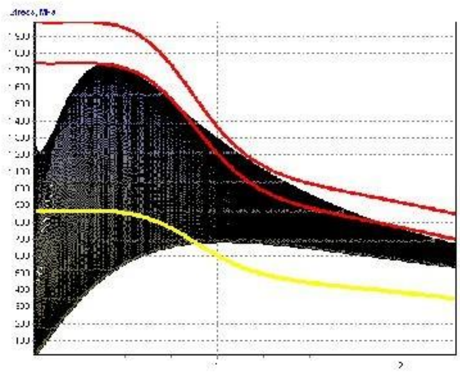

Sigma_von Misses and Rm(HRC), σ02(HRC), τ adm. for 0 mm – grinding

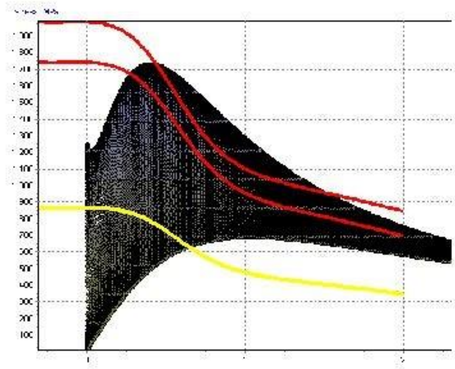

Sigma_von Misses and Rm(HRC), σ02(HRC), τ adm. for 0.31 mm –grinding

Fig. 10. Grinding effect in superimposed model for C45 m, 16 KHz, f=0.52, Dw=20 mm

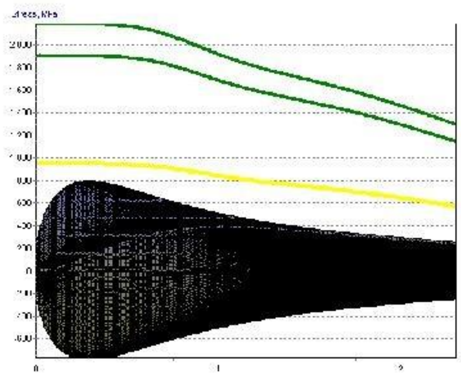

Sigma_tau and Rm(HRC), σ02(HRC), τ adm. for 0 mm – grinding

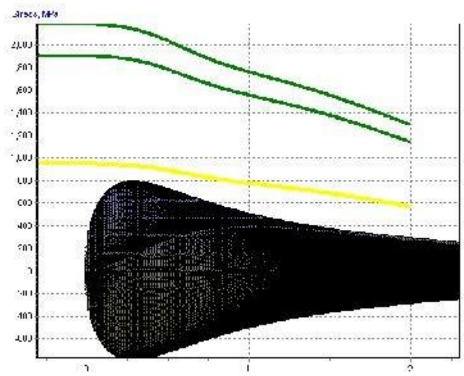

Sigma_tau and Rm(HRC), σ02(HRC), τ adm. for 0.31 mm – grinding

Fig. 11. Grinding effect in superimposed model for C45 max, 16 KHz, f=0.52, Dw=20 mm

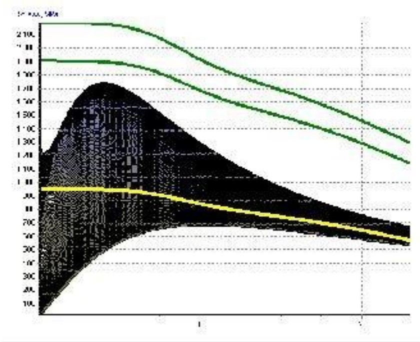

Sigma_von Misses and Rm (HRC), σ02 (HRC), τ adm. for 0 mm – grinding

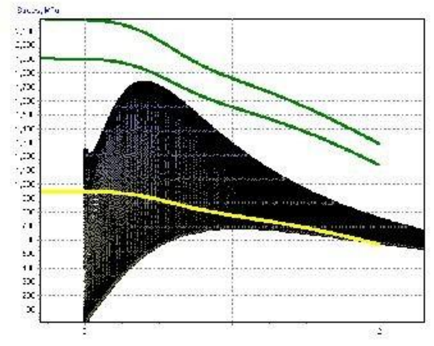

Sigma_von Misses and Rm (HRC), σ02(HRC), τ admi. for 0.31 mm – grinding

Fig. 11. (continuing) Grinding effect in superimposed model
for C45 max, 16 KHz, f=0.52, Dw=20 mm

2. CONCLUSIONS

This mathematical model is useful for slewing rings constructors in order to correctly choose a ball diameter according to the material type and hardness grade and shows the potential risk in the subsurface. This model can specify where will start the raceway problems and will indicate the allowed limits of the material. It also points out the maximum grinding deep in raceway as function of the induction machine parameters. The manufacturing process of slewing rings at SIRCA S.A takes into account all these parameters and a link between theory and practice is done to assure the customers of the correct construction of demanded slewing rings.

REFERENCES

1. **Harris T.A.**, 1991, Rolling bearing analysis, 3rd edition, Wiley-Interscience.
2. **Johnson K.L,** 1985, Contact Mechanics, Cambridge University Press.
3. ******* Thyrofort. Heat treatable steels, EDELSTAHL WITTEN-KREFELD GMBH, available on-line (8.11.2012): http://www.dew-stahl.com/.
4. **Cibaldri C.,** 2006, I Criteri di scelta e di trattamento degli acciai da costruzione e da utensili, volumes 1, 2, 3, AQM.
5. *** ASM Handbook 2005, Volume 1 – Properties and Selection: Irons, Steels, and High Performance Alloys.
6. **Jacot A.,** 1997, Modelisation des transformations de phase a l’etat solide dans les aciers et applications au traitement thermique par induction, PhD These, Laussan
7. *** Sirca - Eng - Electronic -V2010-Ok slewing rings bearing catalogue bearing manufacturer, available on-line (8.11.2012): http://www.scribd.com/doc/29647117/Sirca-Eng-Electronic-V2010-Ok-slewing-rings-bearing-catalogue-bearing-manufacturer.
8. *** Slewing rings, available on-line (8.11.2012): www.rimaspa.com
9. **Rezmiers D.,** 2003, Research about Dynamics and Kinematics Optimization of the Spherical Roller Bearings, Iasi, Romania.
10. **Ledrappier F.,** 2005, Méthodologie d’étude pour optimiser la tenue en fatigue superficielle de dépôts minces – Phd Thèse – L’école centrale de Lyon.
11. **Raport de autoevaluare.** Perioada 2006 – octombrie 2010, available on-line (7.09.2012): www.sirca.com.ro.